18. Okamoto M, Suzuki Y, Shirai K, *et al*: Effect of radiation on the development of immature hippocampal neurons in vitro. Radiat Res 172: 718-724, 2009.
19. Shirai K, Mizui T, Suzuki Y, Kobayashi Y, Nakano T and Shirao T: Differential effects of x-irradiation on immature and mature hippocampal neurons in vitro. Neurosci Lett 399: 57-60, 2006.
20. Goslin K, Asmussen H and Banker G: Rat hippocampal neurons in low-density culture. In: Banker G and Goslin K (eds): Culturing Nerve Cells. Second edition. The MIT Press, Cambridge, MA, pp339-370, 1998.
21. Seaberg RM and van der Kooy D: Adult rodent neurogenic regions: the ventricular subependyma contains neural stem cells, but the dentate gyrus contains restricted progenitors. J Neurosci 22: 1784-1793, 2002.
22. Hellström NA, Björk-Eriksson T, Blomgren K and Kuhn HG: Differential recovery of neural stem cells in the subventricular zone and dentate gyrus after ionizing radiation. Stem Cells 27: 634-641, 2009.

Cellular localization and dendritic function of rat isoforms of the SRF coactivator MKL1 in cortical neurons

Mitsuru Ishikawa[a,*], Jun Shiota[a,*], Yuta Ishibashi[a,*], Tomoyuki Hakamata[a,*], Shizuku Shoji[a], Mamoru Fukuchi[a], Masaaki Tsuda[a], Tomoaki Shirao[b], Yuko Sekino[c], Jay M. Baraban[d] and Akiko Tabuchi[a]

The ability of megakaryoblastic leukemia 1 (MKL1) to function as a serum response factor (SRF) coactivator is regulated through its association with G-actin. In the cytoplasm, MKL1 binds to G-actin through RPXXXEL (RPEL) motifs. However, dissociation of MKL1 from G-actin triggers its translocation into the nucleus where it stimulates SRF-mediated gene expression. Previous characterization of rat MKL1 gene products has identified several isoforms: full-length MKL1, basic, SAP, and coiled-coil domain (BSAC), MKL1-elongated derivative of yield (MELODY), and MKL1met. In this study, we have investigated whether these MKL1 isoforms, which contain different numbers of RPEL motifs, differ in their subcellular localization, transcriptional activity, and effect on dendritic number and axonal length. Immunofluorescent staining of cultured cortical neurons expressing individual FLAG-tagged MKL1 isoforms indicated that all MKL1 isoforms are present in both the cytoplasm and the nucleus. However, MKL1met, which contains two RPEL motifs, shows enhanced nuclear staining compared with the other three isoforms, full-length MKL1, basic, SAP, and coiled-coil domain, and MKL1-elongated derivative of yield, which contain three RPEL motifs. Consistent with its preferential nuclear localization, overexpression of MKL1met, but not other isoforms, increases SRF-mediated transcriptional responses and reduces the number of dendrites. In contrast to the inhibitory effect of MKL1met on dendritic number, axonal length is not affected by overexpression of any of the MKL1 isoforms. These findings suggest that the subcellular localization of MKL1 isoforms, which is mediated by the number of actin-binding RPEL motifs, regulates their effect on SRF-mediated gene expression and dendritic morphology. *NeuroReport* 25:585–592 © 2014 Wolters Kluwer Health | Lippincott Williams & Wilkins.

NeuroReport 2014, 25:585–592

Keywords: dendritic morphology, gene expression, megakaryoblastic leukemia, serum response factor

[a]Laboratory of Molecular Neurobiology, Graduate School of Medicine and Pharmaceutical Sciences, University of Toyama, Toyama, [b]Department of Neurobiology and Behavior, Gunma University, Graduate School of Medicine, Maebashi, [c]Division of Pharmacology, Biological Safety Research Center, National Institute of Health Sciences, Tokyo, Japan and [d]Solomon H. Snyder Department of Neuroscience, Johns Hopkins University, School of Medicine, Baltimore, Maryland, USA

Correspondence to Akiko Tabuchi, Laboratory of Molecular Neurobiology, Graduate School of Medicine and Pharmaceutical Sciences, University of Toyama, 2630 Sugitani, Toyama 930-0194, Japan
Tel: +81 76 434 7536; fax: +81 76 434 5048;
e-mail: atabuchi@pha.u-toyama.ac.jp

*Mitsuru Ishikawa, Jun Shiota, Yuta Ishibashi, and Tomoyuki Hakamata equally contributed to the writing of this article.

Received 28 November 2013 **accepted** 4 February 2014

Introduction

Serum response factor (SRF) plays critical roles in pathological and biological processes including brain development and function [1–6]. SRF-mediated gene expression is tightly regulated by SRF binding cofactors, which are classified into at least two families. One family contains the Ets-like transcription factor (Elk1), SRF accessory protein 1 (SAP1)/Elk4, and a newly described Ets transcription factor (Net)/Ets-related protein/SAP2/Elk3 [6]. The other, referred to as the myocardin and megakaryoblastic leukemia (MKL) family, consists of megakaryocytic acute leukemia/MKL1/myocardin-related transcription factor-A/basic SAP and coiled-coil domain (BSAC) and MKL2/MRTF-B [7–11]. The ability of MKL1 to bind to G-actin through its RPXXXEL (RPEL) motifs plays a prominent role in restraining its transcriptional activity. Conversely, actin rearrangement can lead to its dissociation from G-actin allowing it to translocate into the nucleus [12,13]. Accumulating evidence suggests that MKL1 and MKL2 are enriched in the brain [14] and are deeply involved in regulating neuronal migration and morphology [14,15]. Therefore, analyzing the expression and function of MKL family members in neurons might provide novel insights into the impact of SRF-mediated transcription on neuronal morphology and function.

Use of alternative 5′-exons and translation start sites on the MKL1 gene gives rise to multiple MKL1 isoforms [8,12]. Previously, we identified several rat MKL1 transcripts, including full-length MKL1 (FLMKL1), BSAC, and a novel isoform, MKL1-elongated derivative of yield (MELODY), each of which uses a distinct 5′-exon [16]. These three transcripts are enriched in the testis and brain and are differentially regulated during

Supplemental digital content is available for this article. Direct URL citations appear in the printed text and are provided in the HTML and PDF versions of this article on the journal's website (*www.neuroreport.com*).

0959-4965 © 2014 Wolters Kluwer Health | Lippincott Williams & Wilkins

DOI: 10.1097/WNR.0000000000000141

brain development [16]. The deduced exon–intron organization, domain structure, and different N-termini of rat MKL1 transcripts are illustrated in supplementary Fig. 1 (Supplemental Digital Content 1, *http://links.lww.com/WNR/A275*) [16]. Although the N-terminal regions just ahead of the first RPEL motifs are different between BSAC and MELODY, these two transcripts encode proteins that contain three RPEL motifs (Supplementary Fig. 1B and C, Supplemental Digital Content 1, *http://links.lww.com/WNR/A275*) [16]. In contrast, two isoforms are generated from the FLMKL1 transcript through the use of two alternative translational start sites: the upstream site (CTG) yields the FLMKL1 isoform, which has three RPEL motifs, whereas the downstream start site (ATG) yields MKL1met, which contains only two RPEL motifs (Supplementary Fig. 1B and C, Supplemental Digital Content 1, *http://links.lww.com/WNR/A275*) [12,16]. As RPEL motifs bind to G-actin, it is possible that the number of RPEL motifs affect nucleocytoplasmic localization or function of MKL1. In this study, we expressed these four MKL1 isoforms in rat cortical neurons to compare their subcellular localization and impact on SRF-mediated transcription and neuronal morphology.

Materials and methods

Animals

Neurons of pregnant Sprague–Dawley rats used to prepare primary neuronal cultures were purchased from Sankyo Labo Service Corporation Inc. (Tokyo, Japan). All experiments were carried out in accordance with the guidelines of the Animal Care and Experimental Committee of the University of Toyama, Sugitani Campus. The protocols were approved. Every effort was made to minimize suffering, including anesthetizing with pentobarbital (50 mg/kg, intraperitoneal injection).

Plasmids and antibodies

Construction of FLAG-tagged rat MKL1 vectors (FLAG-FLMKL1, FLAG-BSAC, FLAG-MELODY, and FLAG-MKL1met) has been described previously [16]. The expression vector for enhanced green fluorescent protein (GFP; pEGFP-C1) was purchased from Clontech (Mountain View, California, USA). The SRF reporter vector, 3DA-Luc, was generously supplied by Dr R. Treisman (Cancer Research Institute, London, UK) [12,17,18]. The CRE-reporter vector, pCRE-Luc (CRE-Luc), and the SRE reporter vector, pSRE-Luc (SRE-Luc), were purchased from Stratagene (La Jolla, California, USA). An internal control vector, RSV-βgal vector, has been described previously [14].

The following antibodies were used at the indicated dilutions: Alexa Fluor 488 or 594-conjugated anti-rabbit IgG (Life Technologies, Carlsbad, California, USA, A-11008 and A-11012, respectively; 1 : 1000) and Alexa Fluor 488 or 594-conjugated anti-mouse IgG (Life Technologies, A-11001 and A-11005, respectively; 1 : 1000) produced in goats. The following rabbit polyclonal antibodies were used: anti-GFP (Life Technologies, A-11122 or Medical and Biological Laboratories, 598; 1 : 500 or 1 : 1000). The following mouse monoclonal antibodies were used: anti-FLAG (Sigma, St Louis, Missouri, USA, F3165; 1 : 1000), anti-Tau-1 (Chemicon, Temecula, California, USA, MAB3420; 1 : 1000), and anti-MAP2 (Sigma, M4403; 1 : 1000).

Cell culture

Dissociated cortical cell cultures were prepared from rat embryos at embryonic day 17 as described previously [14]. For reporter assays, cells were plated at 2×10^6 cells/well in six-well plates coated with poly-D-lysine (Sigma). For dendritic morphological assays, cells were seeded at a density of $\sim 7 \times 10^5$ cells/well onto 18-mm circular coverslips coated with poly-D-lysine that had been placed in 12-well plates. For measurement of axonal length, cells were seeded onto coverslips as described above at a density of $\sim 3.0 \times 10^5$ cells/well.

Transfection into rat cortical neurons

For analyzing transcriptional activity, cellular localization, and dendritic morphology, rat cortical neurons cultured for 7 days were transfected using the calcium phosphate precipitation method as described previously [14]. According to our previous observation of the expression levels of FLAG-tagged MKL1 isoforms in NIH3T3 cells [16], we adjusted the amounts of the expression vectors used for transfection of neuronal cultures (see figure legends for specific amounts used for each of these plasmids). We evaluated the expression levels by comparing band intensities on western blotting and observed the same expression levels when the ratio of the expression vectors for transfection was empty vector : FLMKL1 : BSAC : MELODY : MKL1met = 2 : 1 : 2 : 1 : 1.5 [16]. The transfection efficiencies of all samples were equal, as the expression of the internal control GFP, which was cotransfected with the FLAG-tagged expression vector, was equal [16].

Immunostaining

The procedures used to process cortical cultures for immunostaining have been described previously [14]. In this experiment, fluoromount (Diagnostic BioSystems, Pleasanton, California, USA) was used to mount coverslips containing cortical cultures onto microscope slides.

Localization of FLAG-tagged MKL1

After immunostaining, immunofluorescence images were acquired using a Zeiss LSM700 confocal microscope (Zeiss, Oberkochen, Germany). Thereafter, the fluorescence intensities of FLAG-MKL1 isoforms in the cytoplasm and the nucleus were measured using LSM Software ZEN (Zeiss). The cytoplasmic signal was captured as the FLAG-derived immunoreactivity in the GFP-positive and 4′,6-diamidino-2-phonylindole (DAPI)-negative areas and the nuclear signal was captured as the FLAG-derived immunoreactivity in the GFP and DAPI double-positive areas. Twenty neurons were examined

Fig. 1

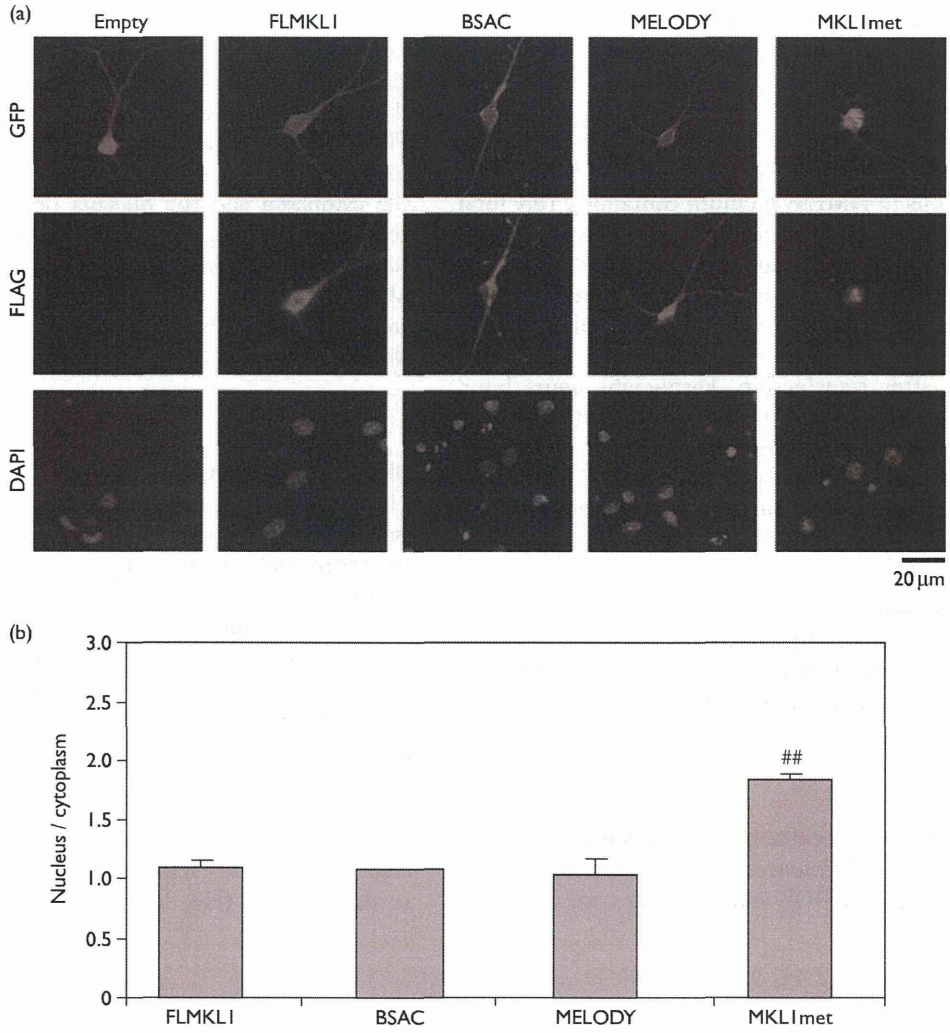

Cellular localization of rat MKL1 isoforms in cortical neurons. (a) Either the empty (empty: 2.0 μg/well), FLAG-tagged FLMKL1 (1.0 μg/well), BSAC (2.0 μg/well), MELODY (1.0 μg/well), or MKL1met (1.5 μg/well) vector was cotransfected with the GFP vector (2.0 μg/well) into rat cortical neurons. To equalize the total amount of vectors (4 μg total/well) used for transfection, the empty vector was added as needed. Cells were fixed 24 h after transfection and stained with anti-GFP antibody (top row), anti-FLAG antibody (middle row), and DAPI (bottom row). Scale bar: 20 μm. (b) The ratio of nuclear/cytoplasmic localization of rat MKL1 isoforms under the experimental conditions shown in (a). Bar graphs represent the mean±SD from three independent experiments ($N=3$). The average value for each experiment was based on evaluation of 20 neurons. The fluorescence intensities of the nucleus and cytoplasm were measured using ZEN software (Zeiss). ##Significance level of $P<0.01$ compared with FLMKL1. BSAC, basic, SAP, and coiled-coil domain; DAPI, 4′,6-diamidino-2-phonylindole; FLMKL1, full-length megakaryoblastic leukemia 1; GFP, green fluorescent protein; MELODY, megakaryoblastic leukemia 1-elongated derivative of yield; MKL1met, megakaryoblastic leukemia 1 met.

in each of three independent experiments used for statistical analyses.

Reporter assay

Transcriptional activity was monitored on the basis of either firefly luciferase or β-galactosidase activity as described previously [14]. In brief, cortical neurons, grown on the six-well plates, were transfected with vectors (4 μg/well) in the following ratios: reporter vector: expression vector = 1 : 3 and firefly luciferase : β-galactosidase = 5 : 1. Cell lysates from cortical neurons were prepared using Tropix lysis solution (Applied Biosystems, Foster City, California, USA). Firefly luciferase and β-galactosidase activities were measured by mixing the cell lysates and substrates. The transcriptional activity was calculated by dividing firefly luciferase activity by β-galactosidase activity.

Morphological analysis

To monitor dendritic morphology of cortical neurons, Sholl analysis was carried out for evaluating dendritic complexity. Detailed procedures have been described

previously [14]. For measurement of axonal length, a 500-μl cell suspension of cortical neurons (5.0×10^6 cells), freshly prepared from rat embryos, was used for electroporation-mediated transfection using the Amaxa Rat Neuron Nucleofector Kit (Lonza, Allendale, New Jersey, USA). FLAG-tagged MKL1 vectors were cotransfected with the GFP vector into rat cortical neurons by electroporation at 0 DIV. Immediately after transfection, $\sim 4.0 \times 10^5$ cells in DMEM medium containing 10% fetal calf serum with 100 μg/ml kanamycin sulfate were seeded onto the poly-D-lysine-coated 18-mm circular coverslips, onto which 3.0×10^5 cells were already preseeded (total cell number: 7.0×10^5 cells) in 12-well plates. The medium was changed to B27-containing neurobasal medium 3 h after transfection. Forty-eight hours later, cells were fixed and stained with anti-GFP and anti-Tau-1 antibodies and DAPI. ImageJ software (National Institute of Health, Bethesda, Maryland, USA) was used for the measurement of axonal length by tracing Tau-1 and GFP double-positive processes from the cell body.

Statistical analysis

Statistical significance of treatment effects was analyzed by one-way analysis of variance with the Tukey–Kramer post-hoc test. The number of samples is provided in each figure legend.

Results

Nuclear/cytoplasmic localization of rat MKL1 isoforms

To examine possible differences between the localization of FLMKL1, BSAC, MELODY, and MKL1met, we compared the nuclear and cytoplasmic localization of the MKL1 isoforms in rat cortical neurons. FLAG-tagged MKL1 isoforms were cotransfected into cortical neurons with a GFP expression vector, and their nuclear and cytoplasmic localization was quantified (Fig. 1a). As shown in Fig. 1b, the ratio of nuclear/cytoplasmic localization was ~1.0 for FLMKL1, BSAC, and MELODY isoforms, indicating that comparable levels of these three isoforms were localized to the cytoplasm and the nucleus (left three lanes 1–3). In contrast, the ratio of nuclear/cytoplasmic localization of MKL1met was significantly higher than that of the other MKL1 isoforms tested (Fig. 1b; lane 4, $P < 0.01$ compared with FLMKL1). Thus, the nuclear localization of MKL1met was the highest of all four isoforms.

SRF coactivator function of rat MKL1 isoforms

Next, we checked the SRF coactivator function of MKL1 isoforms in cortical neurons (Fig. 2a–c). To detect SRF transcriptional activity, we used the 3DA-Luc reporter vector, which has three SRF binding sites but is devoid of ternary complex factor binding sites [12,17,18], and the SRE reporter vector (5 × SRE-Luc), which has five SRF binding sites. All four MKL1 isoforms increased SRF-mediated transcriptional responses with MKL1met showing a stronger effect than the other three isoforms in cortical neurons (Fig. 2a and b; $^*P < 0.05$ vs. empty; $^{**}P < 0.01$ vs. empty; $^{\#\#}P < 0.01$ vs. FLMKL1). In contrast, all four MKL1 isoforms did not activate cAMP response element-mediated transcription significantly in cortical neurons (Fig. 2c; $P > 0.05$).

Fig. 2

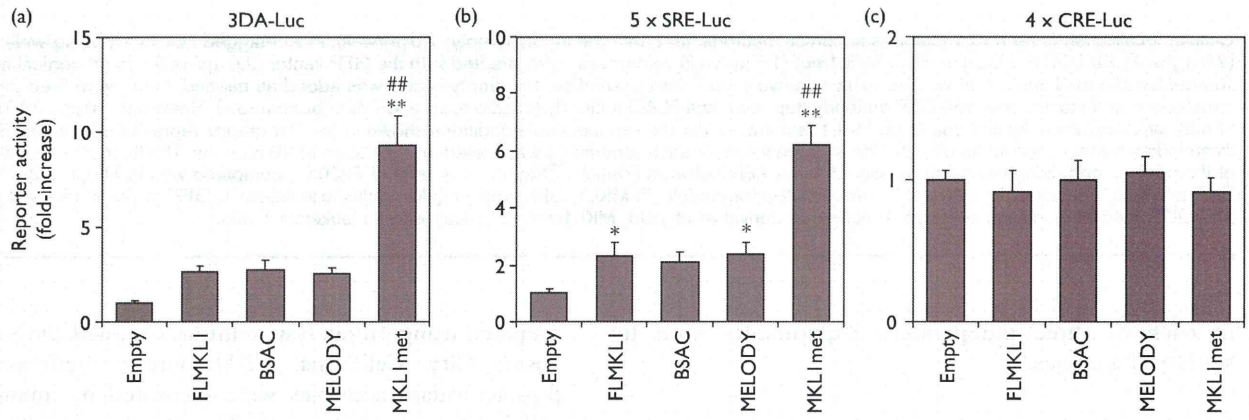

Effects of MKL1 isoforms on SRF-mediated and CREB-mediated transcriptional responses in rat cortical neurons. (a–c) Either the empty (empty: 3.0 μg/well), FLAG-tagged FLMKL1 (1.5 μg/well), BSAC (3.0 μg/well), MELODY (1.5 μg/well), or MKL1met (2.25 μg/well) vector was cotransfected with the firefly luciferase vector indicated [(a) 3DA-Luc, (b) 5 × SRE-Luc, (c) 4 × CRE-Luc, 1.0 μg/well] and the β-galactosidase reporter vector RSV-βgal (0.2 μg/well) into cortical neurons at 7 DIV. Forty-eight hours later, luciferase and β-galactosidase activities were measured. Bar graphs represent the mean±SD [(a) $N=4$; (b) $N=4$; (c) $N=3$] from at least three to four samples. $^*P<0.05$ (vs. empty), $^{**}P<0.01$ (vs. empty), $^{\#\#}P<0.01$ (vs. FLMKL1). BSAC, basic, SAP, and coiled-coil domaim; CRE, cAMP response element; CREB, cAMP response element-binding protein; FLMKL1, full-length megakaryoblastic leukemia 1; GFP, green fluorescent protein; MELODY, megakaryoblastic leukemia 1-elongated derivative of yield; MKL1met, megakaryoblastic leukemia 1 met; SRE, serum response element.

Fig. 3

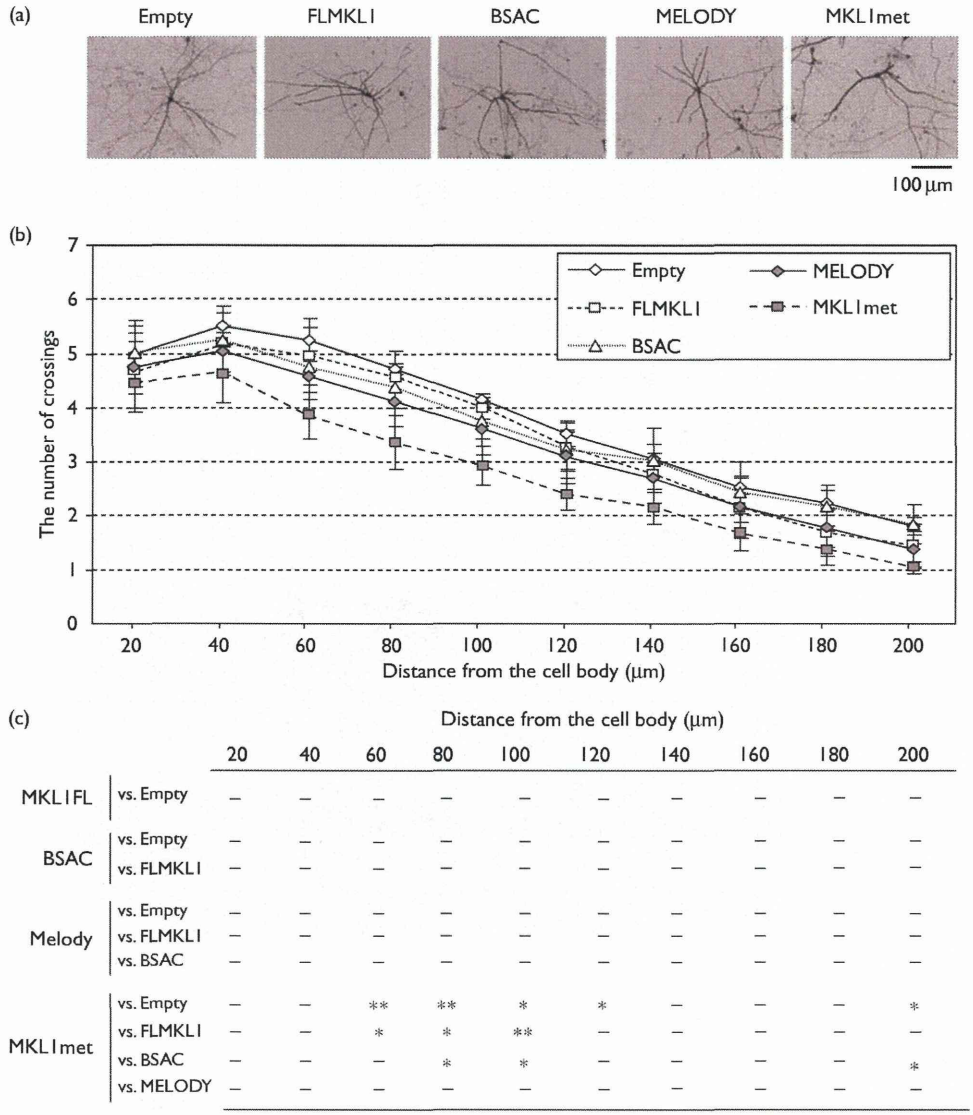

Dendritic morphology of cortical neurons expressing rat MKL1 isoforms. (a) Either the empty (Empty: 2.0 μg/well), FLAG-tagged FLMKL1 (1.0 μg/well), BSAC (2.0 μg/well), MELODY (1.0 μg/well), or MKL1met (1.5 μg/well) vector was cotransfected with the GFP vector (2.0 μg/well) into rat cortical neurons at 7 DIV. To adjust the total amount of vectors (4 μg total/well) for transfection, the empty vector was added as needed. Forty-eight hours later, cells were fixed for immunostaining. Images shown were first converted to gray scale and then transformed into negative images. The images were adjusted as follows: brightness −70%. (b) Dendritic complexity analyzed under the experimental conditions shown in (a). Graphs represent the mean±SD from four independent experiments ($N=4$). In each experiment, a minimum of 20 neurons were monitored to obtain the average value. (c) Statistical significance of Sholl analysis in (b). *$P<0.05$, **$P<0.01$. BSAC, basic, SAP, and coiled-coil domain; FLMKL1, full-length megakaryoblastic leukemia 1; GFP, green fluorescent protein; MELODY, megakaryoblastic leukemia 1-elongated derivative of yield; MKL1met, megakaryoblastic leukemia 1 met.

Taken together, these findings suggest that the increased ability of MKL1met to drive SRF-mediated transcription may be because of its higher level of nuclear localization.

Neuronal morphology of cortical neurons expressing rat MKL1 isoforms

Previous studies have shown that MKL1 affects neuronal morphology [14,18]. Accordingly, we examined the effect of rat MKL1 isoforms on the morphology of cortical neurons. Cortical neurons were immunostained after being cotransfected with expression vectors for GFP and one of the FLAG-tagged MKL1 isoforms (Fig. 3). To examine the effect of MKL1 isoforms on dendritic morphology, we carried out Sholl analysis (Fig. 3b). Compared with the control, overexpression of FLMKL1, BSAC, and MELODY had little effect on dendritic number (Fig. 3b; $P > 0.05$). In contrast, MKL1met decreased dendritic number (Fig. 3b and c; *$P < 0.05$

Fig. 4

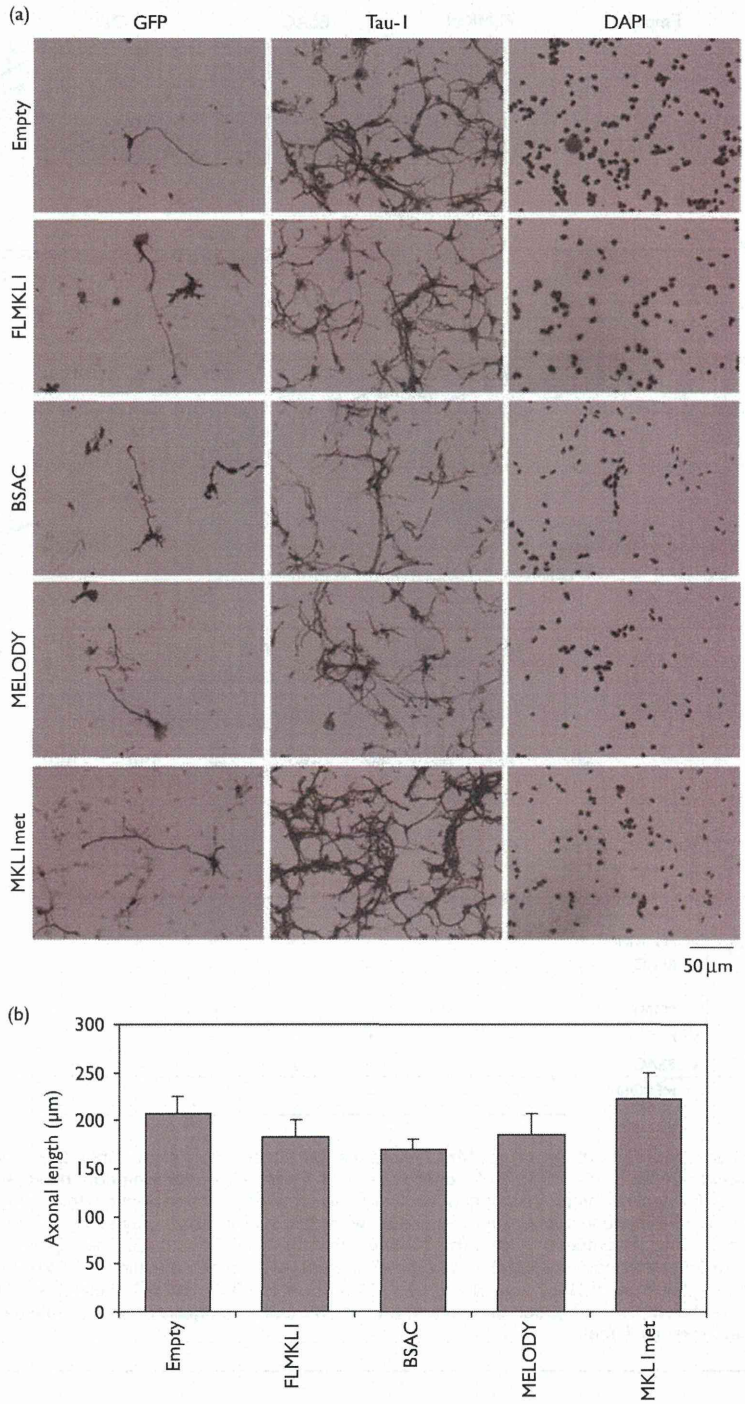

Axonal length of rat cortical neurons expressing MKL1 isoforms. (a) Either the empty (empty: 2.0 μg/well), FLAG-tagged FLMKL1 (1.0 μg/well), BSAC (2.0 μg/well), MELODY (1.0 μg/well), or MKL1met (1.5 μg/well) vector was cotransfected with the GFP vector (2.0 μg/well) into rat cortical neurons using electroporation at 0 DIV. To equalize the total amount of vectors (4 μg total/well) used for transfection, the empty vector was added as needed. Immunostaining and morphological analysis are described in the Materials and methods section. Images shown here were converted to gray scale and then adjusted as follows: brightness −40% and contrast −40%. (b) Axonal length analyzed under the experimental conditions shown in (a). ImageJ software (National Institute of Health) was used for the measurement of axonal length by tracing Tau-1 and GFP double-positive processes from the cell body. Graphs represent the mean±SD from three independent experiments ($N=3$). At least 20 neurons were measured in each experiment. BSAC, basic, SAP, and coiled-coil domain; FLMKL1, full-length megakaryoblastic leukemia 1; GFP, green fluorescent protein; MELODY, megakaryoblastic leukemia 1-elongated derivative of yield; MKL1met, megakaryoblastic leukemia 1 met.

vs. empty at 100, 120, 200 μm; $*P < 0.05$ vs. FLMKL1 at 60, 80 μm; $*P < 0.05$ vs. BSAC at 80, 100, 200 μm; $*P < 0.01$ vs. empty at 60, 80 μm; $*P < 0.01$ vs. FLMKL1 at 100 μm). We also confirmed that mouse MKL1met exerted similar effects on dendritic number following transfection of rat cortical neurons (data not shown). In contrast, we found that none of the four MKL1 isoforms affected axonal length of cortical neurons significantly (Fig. 4a and b; $P > 0.05$). Taken together, these findings suggest that the most prominent effects of MKL1 isoforms on neuronal morphology are shown by the MKL1met isoform, which selectively affects dendritic morphology.

Discussion

By comparing the localization and function of rat MKL1 isoforms in cultured cortical neurons, we have found that MKL1met differs from the other three isoforms in three ways: increased nuclear localization (Fig. 1), enhanced SRF coactivation (Fig. 2), and reduced dendritic complexity (Fig. 3). As a prominent difference between MKL1 met and the other isoforms is that it contains one less RPEL motif, it is tempting to suggest that the selective effects of MKL1met are due to the reduced number of RPEL motifs. Five G-actin monomers are thought to bind to three RPEL motifs in MKL1 [19]. Therefore, the number of G-actin subunits bound to MKL1met may be lesser than that bound to FLMKL1, BSAC, and MELODY. As free MKL1, released from G-actin, has been shown to be able to translocate into the nucleus in several cell types, it is reasonable to infer that because MKL1met would be bound to fewer G-actin molecules, it may move into the nucleus more readily than the other three MKL1 isoforms in cortical neurons. G-actin also affects the nuclear export and SRF coactivator function of MKL1; interaction of MKL1 with G-actin promotes nuclear export of the complex and G-actin-bound MKL1 is inactive in the nucleus [20]. Thus, the reduced number of RPEL motifs in MKL1met may increase its SRF coactivator function by reducing the suppressive effects of G-actin and increasing its localization in the nucleus. It would be interesting to test in future studies the prediction that deletion of RPEL motifs from BSAC or MELODY would increase nuclear localization and SRF-mediated transcription, as well as decrease dendritic number.

Overexpression of MKL1met reduced the dendritic complexity of cortical neurons (Fig. 3). In contrast, overexpression of MKL*2* in cortical neurons increased dendritic complexity [14]. Although overexpression studies indicate that both MKL1met and MKL*2* act as SRF coactivators (Ishikawa and colleagues [14,16] and this study), paradoxically, they have opposite effects on dendritic morphology. Taken together, these findings suggest that MKL1- and MKL*2*- target different genes that play opposite roles in dendritic morphology. However, RNAi-mediated MKL1 and MKL*2* knockdown showed the same morphological change, that is, a reduction in dendritic complexity of cortical neurons [14]. Analysis of MKL1/MKL*2* double-knockout mice also showed that MKL1 and MKL*2* play redundant roles in neuronal migration and neurite outgrowth [15]. To investigate whether MKL1 and MKL*2* play differential or redundant roles in brain function, identification of the target genes of MKL1 and/or MKL*2* in neurons would likely be helpful.

In summary, we examined the cellular localization and function of rat MKL1 isoforms in neurons and found that MKL1met, which has fewer RPEL motifs than the other three isoforms, shows increased nuclear localization and SRF coactivator function. Further, this isoform reduces dendritic complexity, whereas the other isoforms did not affect this aspect of neuronal morphology. Our previous study reported that rat MKL1 transcripts show differential patterns of expression in the developing and the mature brain [16]. Further studies are warranted to assess whether different MKL1 isoforms influence the expression of different genes. Taken together, these studies suggest that the varying patterns of expression of multiple MKL1 isoforms with distinctive functional properties contribute to the rich heterogeneity in neuronal morphology found in the developing and the adult brain.

Acknowledgements

The authors thank Dr T. Ohtsuka (University of Yamanashi, Japan) for helpful comments on this manuscript.

This study was supported by a grant-in-aid from the Ministry of Education, Culture, Sports, Science, and Technology of Japan (project number: 17790055, 19790052, and 22590080, A.T.; 20390023, M.T.; 23890065, M.I.) and by research grants from the Hayashi Memorial Foundation for Female Natural Scientists (A.T.), Foundation of the first Bank of Toyama (A.T.), Takeda Science Foundation (A.T.), Narishige Neuroscience Research Foundation (A.T.), and the Research Foundation for Pharmaceutical Sciences (A.T.).

Conflicts of interest

There are no conflicts of interest.

References

1 Miano JM. Role of serum response factor in the pathogenesis of disease. *Lab Invest* 2010; **90**:1274–1284.
2 Ramanan N, Shen Y, Sarsfield S, Lemberger T, Schütz G, Linden DG, *et al.* SRF mediates activity-induced gene expression and synaptic plasticity but not neuronal viability. *Nat Neurosci* 2005; **8**:759–767.
3 Etkin A, Alarcon JM, Weisberg SP, Touzani K, Huang YY, Nordheim A, *et al.* A role in learning for SRF: deletion in the adult forebrain disrupts LTD and the formation of an immediate memory of a novel context. *Neuron* 2006; **50**:127–143.
4 Alberti S, Krause SM, Kretz O, Philippar U, Lemberger T, Casanova E, *et al.* Neuronal migration in the murine rostal migratory stream requires serum response factor. *Proc Natl Acad Sci USA* 2005; **102**:6148–6153.
5 Knöll B, Kretz O, Fiedler C, Alberti S, Schütz G, Frotscher M, *et al.* Serum response factor controls neuronal circuit assembly in the hippocampus. *Nat Neurosci* 2006; **9**:195–204.

6 Buchwalter G, Gross C, Wasylyk B. Ets ternary complex transcription factors. *Gene* 2004; **324**:1–14.

7 Wang DZ, Li S, Hockmeyer D, Sutherland L, Wang Z, Schratt G, *et al.* Potentiation of serum response factor activity by a family of myocardin-related transcription factors. *Proc Natl Acad Sci USA* 2002; **99**:14855–14860.

8 Sasazuki T, Sawada T, Sakon S, Kitamura T, Kishi T, Okazaki T, *et al.* Identification of a novel transcriptional activator, BSAC, by a functional cloning to inhibit tumor necrosis factor-induced cell death. *J Biol Chem* 2002; **277**:28853–28860.

9 Selvaraj A, Prywes R. Megakaryoblastic leukemia-1/2, a transcriptional co-activator of serum response factor, is required for skeletal myogenic differentiation. *J Biol Chem* 2003; **278**:41977–41987.

10 Cen B, Salvaraj A, Prywes R. Myocardin/MKL family of SRF coactivator: key regulators of immediate early and muscle specific gene expression. *J Cell Biochem* 2004; **93**:74–82.

11 Pipes GC, Creemers EE, Olson EN. The myocardin family of transcriptional coactivators: versatile regulators of cell growth, migration and myogenesis. *Genes Dev* 2006; **20**:1545–1556.

12 Miralles F, Posern G, Zaromytidou AI, Treisman R. Actin dynamics control SRF activity by regulation of its coactivator MAL. *Cell* 2003; **113**:329–342.

13 Medjkane S, Perez-Sanchez C, Gaggioli C, Sahai E, Treisman R. Myocardin-related transcription factors and SRF are required for cytoskeletal dynamics and experimental metastasis. *Nat Cell Biol* 2009; **11**:257–268.

14 Ishikawa M, Nishijima N, Shiota J, Sakagami H, Tsuchida K, Mizukoshi M, *et al.* Involvement of the SRF coactivator megakaryoblastic leukemia in the activin-regulated dendritic complexity of rat cortical neurons. *J Biol Chem* 2010; **285**:32734–32743.

15 Mokalled MH, Johnson A, Kim Y, Oh J, Olson EN. Myocardin-related transcription factors regulate the Cdk5/Pctaire 1 kinase cascade to control neurite outgrowth, neuronal migration and brain development. *Development* 2010; **137**:2365–2374.

16 Ishikawa M, Shiota J, Ishibashi Y, Hakamata T, Shoji S, Fukuchi M, *et al.* Identification, expression and characterization of rat isoforms of the SRF coactivator MKL1. *FEBS Open Bio* 2013; **3**:387–393.

17 Tabuchi A, Estevez M, Henderson JA, Marx R, Shiota J, Nakano H, *et al.* Nuclear translocation of the SRF co-activator MAL in cortical neurons: role of RhoA signaling. *J Neurochem* 2005; **94**:169–180.

18 Shiota J, Ishikawa M, Sakagami H, Tsuda M, Baraban JM, Tabuchi A. Developmental expression of the SRF co-activator MAL in brain: role in regulating dendritic morphology. *J Neurochem* 2006; **98**:1778–1788.

19 Mouilleron S, Langer CA, Guettler S, McDonald NQ, Treisman R. Structure of a pentavalent G-actin MRTF-A complex reveals how G-actin controls nucleocytoplasmic shuttling of a transcriptional coactivator. *Sci Signal* 2011; **4**:ra40.

20 Vartiainen MK, Guettler S, Larijani B, Treisman R. Nuclear actin regulates dynamic subcellular localization and activity of the SRF cofactor MAL. *Science* 2007; **316**:1749–1752.

海馬における記憶再生のメカニズム

高木夕貫（たかぎゆう） 東京大学大学院薬学系研究科薬品作用学教室
杉山弘樹（すぎやまひろき） 同
池谷裕二（いけがやゆうじ） 同 教授

夢見る脳スライス

記憶するときに活動したニューロンを人工的に活性化させると強制的に記憶が思い出されることが，2012年に利根川進らの研究によって明らかにされている[1]．この事実は，記憶に関わったニューロンそのものが「記憶痕跡」であることを意味している．一方 現実の脳では，この記憶痕跡は（人工的な刺激でなく）自然に再生（リプレイ）される．

近年の研究により，記憶痕跡の再生は「鋭波」に生じると考えられている[2~5]．鋭波はノンレム睡眠中や安静時に頻繁に観察される脳波の一種で，記憶や学習を司る脳部位である海馬から発生する[6]．鋭波は，形成されたばかりの新しい記憶を脳回路に長期定着させるために重要な働きを担っていると考えられている[7~10]．

従来のような切片化されたin vitro脳標本を観察する手法では，記憶のリプレイのような“生きたままの動物の脳”で起こる現象について明らかにすることは不可能であった．また，記憶をリプレイする仕組みを明らかにするためには，記憶に関わったニューロンと，そうでない多数のニューロンとを区別する必要がある．そこで今回，これらを区別できる特殊な遺伝子改変*Arc-dVenus*マウスの標本を用いて蛍光タンパク質で生きたまま標識し[11]，その後にマウスから海馬を取り出し，スライス標本を作成した[12]．

まず，このスライス標本が鋭波を自然に生じることがわかった（図1）．つまり，取り出された海馬は自然と「睡眠中」に類似した状態になる．いわば，かつてマウスの頭の中にあった頃の記憶を，海馬のスライス標本になってもリプレイさせる（≒夢見る）ことができるというわけである．この「夢見る脳スライス」の発見を弾みとして，「では一体，何がこの記憶のリプレイを引き起こしているのか」「記憶に関わるニューロンと関わっていないニューロンとでは何が異なるのか」という重要な問いを追求できるようになった．

記憶に関連した細胞集団は「鋭波」発生に寄与

さらに重要なことに，眠っている海馬のスライス標本が鋭波を発生している最中に，記憶に関わったニューロンが活性化されていることがわかった．記憶に関わったニューロン（dVenus陽性細胞）と，そうでない多数のニューロン（dVenus陰性細胞）とを区別しながら活動を観察するために，独自に開発した特殊なカルシウム蛍光指示薬CaSiR-1を用いて[13]カルシウムイメージングを行なった（図2A）．すると，記憶に関わったニューロンのほうが，そうでないニューロンに比べて，鋭波が発生している時に活動しやすくなっていることが判明した（図2B）．これは，鋭波が発生している時には正に記憶のリプレイが起こっていることを意味している．この記憶のリプレイ現象はLTPの維持過程を阻害することで観察されなくなった（図2C）．以上の結果から，記憶はLTPによって痕跡として脳回路に保存されることでリプレイされることが示唆される．

抑制と興奮のシグナルのバランスによって記憶のリプレイが生じる

鋭波に参加するニューロンはどのようにして選ばれるのだろう．これを知るために，海馬CA1野切片において発生する「鋭波」を観察すると同時に，各錐体ニューロンが鋭波発生時に受ける興奮性シグナルおよび抑制性シグナルのシナプス入力をパッチクランプ記録によって観察した．この観察により，記憶のリプレイに関係するニューロンでは興奮性シグナルと抑制性シグナルのバランスが興奮性側にシフトしていることが判明した．さらに，ニューロンに人工的なシグナルを注入し，鋭波が起こっている際の神経活動のシミュレーションを行うと，興奮・抑制のバランスが興奮性側にシフトしているシグナルを受けることが，ニューロンの活動を再現よく引き起こすことの原因であることも明らかになった．

次に，鋭波の大きさと興奮性・抑制性シグナルとの関係を調べたところ，一つひとつのニューロンが受け取る興奮性シグナルの値はバラエティ豊かで個性的である一方，抑制性シグナルの値は鋭波の大きさ，つまりCA1野回路内の興奮性シグナルの平均レベルを反映することが判明した．この均一な抑制性シグナルの起源として，抑制性介在ニューロンの一種であるパルバルブミン陽性インターニューロンに着目した．これらのニューロンの活動を観察したところ，パルバルブミン陽性インターニューロンは脳回路内の興奮性シグナルを網羅的に受け取り，興奮性レベルを検知してそれに合わせた出力を行うことで，まわりのニューロンに均一な抑制性シグナルを送っていることが示唆された．

今回の実験結果から，以下のような流れで記憶が再生されると示唆される（図3）．記憶がつくられる時に活動したニューロンではLTPが起こり，上流のニューロン集団との結合性が高まる．そのため記憶に関わったニューロンは平均よりも大きな

0289-0585/15/¥500/論文/JCOPY